Sedimentology (1997) **44,** 959–970

Intermittent saltation

J. E. STOUT and T. M. ZOBECK
USDA/Agricultural Research Service, Lubbock, TX 79401, USA (E-mail: jstout@mail.csrl.ars.usda.gov; tzobeck@mail.csrl.ars.usda.gov)

ABSTRACT

During a typical wind erosion event, large variations in wind strength produce temporal variations in saltation activity. The focus of this paper is on a special type of unsteady behaviour – intermittent saltation – a process characterized by bursts of blowing soil interspersed with periods of inactivity. We report here measurements from a field study designed to measure intermittent saltation during three separate 1-h periods. Our measurements show that natural wind erosion events consist of intermittent bursts of blowing soil often occupying a small fraction of the total time. We have managed to describe the level of intermittency by a simple and universal mathematical expression. We find that the level of intermittency is governed by whether typical wind fluctuations span the gap between the mean wind speed and threshold wind speed. We propose a nondimensional number which expresses the ratio of these velocity scales, called the relative wind strength, and find that the level of intermittency can be described by a simple distribution function of the relative wind strength.

INTRODUCTION

Saltation is often an unsteady process (Lee, 1987; Stockton & Gillette, 1990; Butterfield, 1991). Gusty winds that drive saltating grains produce substantial temporal variations in sediment transport (Jackson, 1996). Often the wind speed falls below that necessary for soil movement, producing a momentary lull followed immediately by strong intermittent gusts producing intense bursts of blowing soil and dust (Porch, 1974). It has been shown that intermittent bursts contribute significantly to the total mass transport and may dominate the process (Heathershaw & Thorne, 1985; Thorne *et al.*, 1989; Butterfield, 1993).

Most recognize that boundary layer winds are highly unsteady. Yet the assumption of steady winds that always remain above threshold is common in numerical modelling efforts (Anderson & Haff, 1991; McEwan & Willetts, 1991; Sørensen, 1991). Past wind tunnel studies, which have helped shape our understanding of the saltation process, also tend to focus on the condition of steady wind and continuous saltation activity (Bagnold, 1941; Kawamura, 1951; Zingg, 1953). One naturally wonders whether the 'continuous saltation' condition reflects the true nature of sediment transport by natural atmospheric winds.

This paper represents an attempt to better define the conditions under which the assumption of steady-state or continuous saltation is valid. We have attempted to quantify the level of intermittency in the aeolian saltation process both experimentally and theoretically. We report measurements of intermittent saltation taken during a field experiment. We demonstrate the relationship between wind strength, threshold, and the resulting level of intermittency and we propose a new method for predicting the level of saltation intermittency in the field.

THEORY OF SALTATION INTERMITTENCY

Classic papers on intermittency by Corrsin (1943), Corrsin and Kistler (1954), and Fiedler and Head (1966) define an intermittency function, γ, that expresses the portion of time a system is active. Here, we adopt a similar notation and define γ_p as the fraction of time during which saltating particles are detected at a given point during a given time period. For example, $\gamma_p = 0{\cdot}25$ means

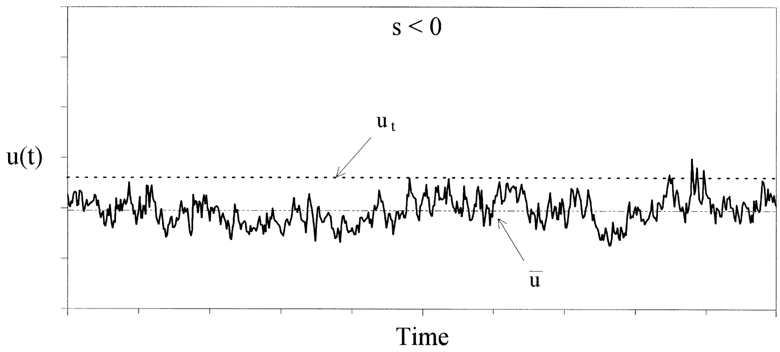

Fig. 1. Schematic illustration for a negative relative wind strength, $s<0$.

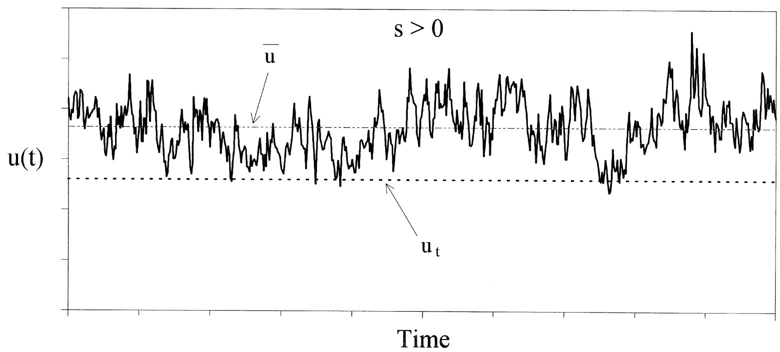

Fig. 2. Schematic illustration for a positive relative wind strength, $s>0$.

that saltation activity was detected for one-quarter of the measurement period. The value of γ_p always falls between 0 and 1 where $\gamma_p=1$ corresponds to the condition of continuous saltation and $\gamma_p=0$ corresponds to the completely inactive condition.

The level of intermittency in the saltation process is governed primarily by whether wind speed fluctuations, characterized by the standard deviation σ, span the gap between the mean wind speed $\overline{u}$ and the threshold wind speed u_t, expressed by $\overline{u}-u_t$. A nondimensional parameter that expresses this *relative wind strength* may be written as

$$s=\frac{\overline{u}-u_t}{\sigma} \tag{1}$$

To demonstrate the relationship between the relative wind strength, s, and the resulting intermittency condition we have sketched three possible situations in Figs 1 through 3.

Figure 1 illustrates the condition of a negative relative wind strength, $s<0$. If s is negative then the mean wind speed is less than threshold. In this case, occasional gusts may exceed threshold and produce blowing soil. As $s\rightarrow-\infty$, saltation activity tends toward zero or $\gamma_p\rightarrow 0$.

Figure 2 illustrates the condition of positive relative wind strength, $s>0$ (the mean wind speed is greater than threshold). Under this condition, saltation will occasionally cease when the wind speed dips beneath threshold. If $s\gg 1$ then wind fluctuations σ are small compared to the velocity difference $\overline{u}-u_t$ and consequently there is a low probability that winds will dip beneath threshold. As $s\rightarrow\infty$, soil transport tends toward continuous saltation activity or $\gamma_p\rightarrow 1$.

Figure 3 illustrates the special case where $\overline{u}=u_t$ or $s=0$. In this case, whenever wind fluctuations exceed the mean wind speed, they also exceed threshold.

In turbulent flows, wind speed fluctuations can be described by a probability density distribution $p(u)$, as depicted schematically in Fig. 4 (Sorbjan, 1989). Here we have denoted the mean wind speed and the threshold wind speed for the soil surface. The probability that a given wind speed will exceed threshold is represented by the shaded area beneath the curve as depicted in Fig. 4.

Since the total area beneath the probability density curve is equal to one, the probability that wind speed will exceed threshold may be expressed as a function of the unshaded area as follows

$$P(u>u_t)=1-\int_{-\infty}^{\frac{u_t-\overline{u}}{\sigma}} p(w)dw, \tag{2}$$

where

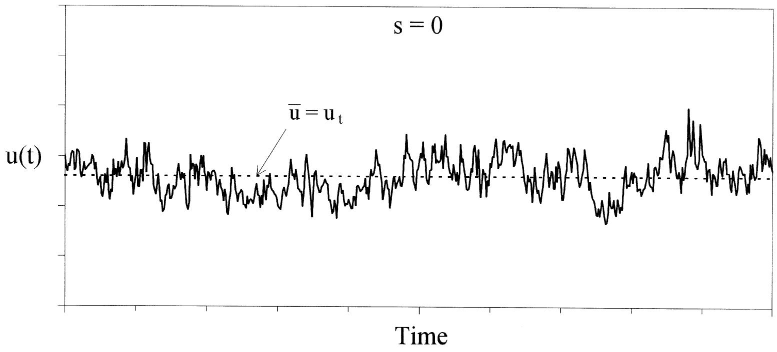

Fig. 3. Schematic illustration for $s=0$.

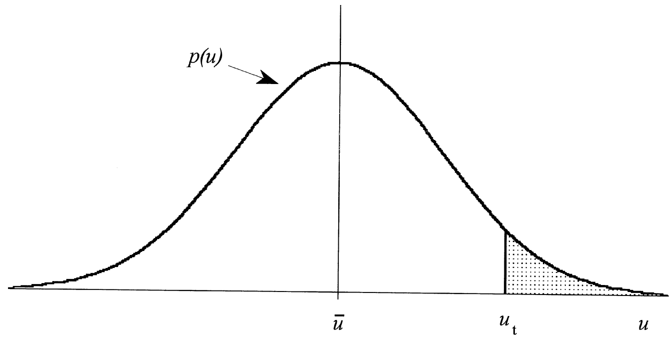

Fig. 4. Schematic drawing of a typical probability density distribution of wind speed. Shaded area represents the probability that wind speed u is greater than threshold u_t.

$$w=\frac{u-\bar{u}}{\sigma}.$$

Let Φ denote a distribution function defined as

$$\Phi\left(\frac{u_t-\bar{u}}{\sigma}\right)\equiv\int_{-\infty}^{\frac{u_t-\bar{u}}{\sigma}} p(w)dw. \tag{3}$$

Note that the argument within the brackets is equal to $-s$, so the probability that the wind speed will exceed threshold may be rewritten in terms of the relative wind strength s as

$$P(u>u_t)=1-\Phi(-s). \tag{4}$$

The distribution function Φ satisfies the property

$$\Phi(-s)=1-\Phi(s). \tag{5}$$

Combining Eqs (4) and (5) yields

$$P(u>u_t)=\Phi(s). \tag{6}$$

The fraction of time that saltation occurs should equal the fraction of time that winds exceeds threshold. Thus,

$$\gamma_p=P(u>u_t), \tag{7}$$

and it follows from Eqs (6) and (7) that

$$\gamma_p=\Phi(s). \tag{8}$$

Equation (8) suggests that the intermittency function γ_p follows a curve defined by the distribution function $\Phi(s)$.

So far we have not defined the form of the distribution function $\Phi(s)$. From Eq. (6), we know that the form of the wind speed distribution governs the form of $\Phi(s)$. Candidate wind distribution forms include the normal distribution (Simmons & Salter, 1934; Townsend, 1947; Kuo & Corrsin, 1971), the Weibull distribution (Weibull, 1951; Justus *et al.*, 1976; Takle & Brown, 1978), and the lognormal distribution (Luna & Church, 1974). Since the proposed theory makes no restrictions as to the form of the wind distribution, any one of these forms could be used here if found appropriate.

It is generally agreed that under ideal conditions of homogeneous and stationary turbulence the distribution of wind fluctuations conforms closely to the normal or Gaussian distribution (Townsend, 1947; Sutton, 1949; Lumley & Panofsky, 1964; Kuo & Corrsin, 1971). Although a truly stationary turbulent field rarely exists in the atmosphere, the assumption of stationarity for nonstationary flows is sometimes acceptable in selected short periods of time, during which changes seem to occur through 'quasi-stationary' states (Sorbjan, 1989). Also, the assumption of homogeneous turbulence is sometimes acceptable

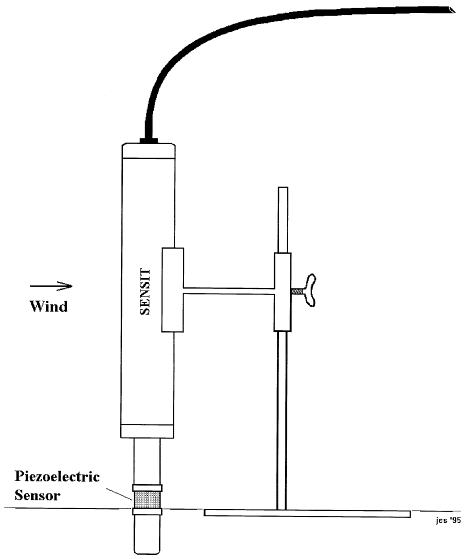

Fig. 5. Schematic drawing of the SENSIT saltation sensor and mounting stand.

at heights sufficiently far from the surface as shown by Maitani, 1979. Thus, it is possible for the wind distribution to be adequately described by the normal distribution despite the fact that the conditions of homogeneous and stationary turbulence are not rigorously satisfied. Nevertheless, it is left to experiment to decide on the proper form for the wind speed distribution which will be calculated directly from measurements of wind speed taken during this field study.

FIELD STUDY

One purpose of this field study was to quantify the fraction of time that a given surface experiences saltation and relate saltation activity to wind and surface conditions. The experiment was conducted on a 40-acre field located within the Southern High Plains just north of Lubbock, Texas (33°41′9·6″N and 101°46′4·8″W). The surface soil type was a sandy loam with 80% sand, 4% silt, and 16% clay. The organic matter content was 0·7%. The surface had been plowed a few months before the experiment creating a series of furrows spaced about one meter apart with their long axes running WSW-ENE (254°). The amplitude of furrows was about 0·2 m. Rainfall had considerably smoothed the surface, producing a crusted layer with loose erodible soil particles perched on top of the crust. Most of the erodible material tended to accumulate at the bottom of the furrows providing multiple line sources of saltation-size grains.

Wind speed was measured by a lightweight fast-responding cup anemometer mounted at a height of 2 m. The responsiveness of such an anemometer is typically given in terms of a distance constant which represents the length of travel of an airstream required for the anemometer to respond to 63% of a step change in wind speed. In this case the distance constant was 2·3 m. The time response of the anemometer can be obtained by dividing the distance constant by the wind speed to obtain the time constant. A wind speed of 10 m s^{-1} yields a time constant of 0·23 s and higher wind speeds reduce the response time. During a typical dust storm within the Southern High Plains it is not unusual for wind speeds to exceed 10 m s^{-1} and so the time constant is sufficiently small to allow sampling at a frequency of 1 Hz.

We used an instrument called SENSIT[1] to monitor saltation activity. SENSIT, shown in Fig. 5, contains a piezoelectric crystal which responds to the impact of saltating grains and outputs a pulse signal proportional to the number of such impacts (Stockton & Gillette, 1990). We sampled the signal from SENSIT each second so that the output represents the number of particles that impact the surface of the piezoelectric crystal each second. Although others have attempted to interpret the signal as a measure of mass flux or momentum (Gillette & Stockton, 1986), we used the signal from SENSIT only to detect the presence of saltating grains.

The sensitivity of the piezoelectric crystal is adjusted in order to primarily respond to the impact of large saltating grains (Stockton & Gillette, 1990). This adjustment reduces the possibility of false readings from wind vibration or electrostatic noise. In addition, fine particles normally follow the airflow around the sensing element. Even if a fine dust speck were to impact the crystal, the momentum transfer would be too low to trigger a pulse.

We completed a series of sensitivity tests of the SENSIT by dropping glass beads from a fixed height onto the sensing element. These tests revealed that the piezoelectric crystal does not respond to particles with momentum less than about 5×10^{-8} N s. Particle momentum is the product of particle mass and velocity, so a small particle moving quickly can have the same

[1]Names are necessary to report factually on available data; however, the USDA neither guarantees nor warrants the standard of the product, and the use of the name by USDA implies no approval of the product to the exclusion of others that may also be suitable.

Table 1. Minimum velocity of a given diameter sand grain (particle density of 2650 kg m^{-3}) that yields a particle momentum of 5×10^{-8} N s.

Diameter (µm)	Mass (kg)	Velocity (m s^{-1})
100	1·39E-09	36·04
150	4·68E-09	10·68
200	1·11E-08	4·50
300	3·75E-08	1·33
400	8·88E-08	0·56
500	1·73E-07	0·29
600	3·00E-07	0·17
700	4·76E-07	0·11
800	7·10E-07	0·07
900	1·01E-06	0·05
1000	1·39E-06	0·04

momentum as a large particle moving slowly. The minimum velocity of a given diameter sand grain (particle density of 2650 kg m^{-3}) that yields a particle momentum of 5×10^{-8} N s is calculated in Table 1. The calculations suggest that it is unlikely that SENSIT responds to particles with diameters less than 100 µm since it is nearly impossible for such grains to attain speeds greater than 36 m s^{-1} during a typical wind erosion event. It appears, however, that SENSIT will respond to particles larger than 150 µm since the required particle speed is reasonably close to typical wind speeds experienced during intense wind erosion events.

As dust can be generated far upwind and transported long distances, the presence of dust is not a reliable indicator of soil movement at a single point whereas saltation activity clearly indicates soil movement at the point of measurement. Thus, the fact that SENSIT ignores the movement of fine particles is a positive feature since the selective signal from SENSIT provides a clear indication of saltation activity at a given point within the field.

SENSIT was mounted so that the lower edge of the sensing crystal was set flush with the eroding surface, as shown in Fig. 5. The cylindrical sensing element extended from the surface to a height of 13 mm and the diameter of the sensing element was 25 mm forming a frontal impact area of 325 mm^2. The number of particle impacts divided by the 1-s sampling interval yields a value of particle impacts per second $p(t)$.

EXPERIMENTAL RESULTS

On 19 April 1995, we recorded data for three 1-h periods between 17:24 and 20:42. The wind direction, 2-m wind speed, and saltation activity are plotted as a function of time in Figs 6, 7 and 8.

The first sampling period, from 17:24–18:24, was characterized by the strongest winds and the most saltation activity. During this 1-h period, the 2-m wind speed ranged from 7·38 to 19·92 m s^{-1} with a mean value of 12·58 m s^{-1} and a standard deviation of 1·93 m s^{-1}. SENSIT recorded a maximum of 90 particle impacts s^{-1}, the largest value recorded during the storm. Despite the high wind velocities, saltation activity accounted for only 944 s out of the 3600-second sampling period or 26% of the total sampling period.

Within the second hour, from 18:42–19:42, the wind weakened and saltation activity decreased significantly. The 2-m wind speed ranged from 6·61 m s^{-1} to 16·46 m s^{-1} with a mean value of 10·72 m s^{-1} and a standard deviation of 1·68 m s^{-1}. SENSIT recorded a maximum value of 37 impacts s^{-1}. Saltation activity accounted for only 207 s out of the 3600-s sampling period or 6% of the second sampling period.

During the third sampling period, from 19:42–20:42, the wind weakened considerably. The wind speed varied from 4·83 m s^{-1} to 14·46 m s^{-1} with a mean value of 8·77 m s^{-1} and a standard deviation of 1·52 m s^{-1}. SENSIT recorded a maximum value of 6 particle impacts s^{-1}. Saltation activity accounted for only 12 s out of a total of 3600 s or 0·33% of the total sampling period.

Overall, the results show a gradual reduction of wind strength with time resulting in increasingly intermittent saltation. For all three 1-h sampling periods, saltation activity accounted for a small fraction of the total time. The largest fraction of time that saltation occurred for any 1-h sampling period was 26% and this value reduced to less than 1% toward the end of the storm.

COMPARISON OF INTERMITTENCY THEORY WITH FIELD DATA

It is possible to test the theory put forward in this paper using the measurements of wind speed and saltation activity taken during this field experiment. Here, we focus on the first two 1-h data collection periods (17:24–18:24 and 18:42–19:42). The level of saltation activity within the third hour (19:42–20:42) was too low to be of significant value.

Each hour was split into 12 5-min periods. Since the sampling frequency was 1 sample s^{-1}

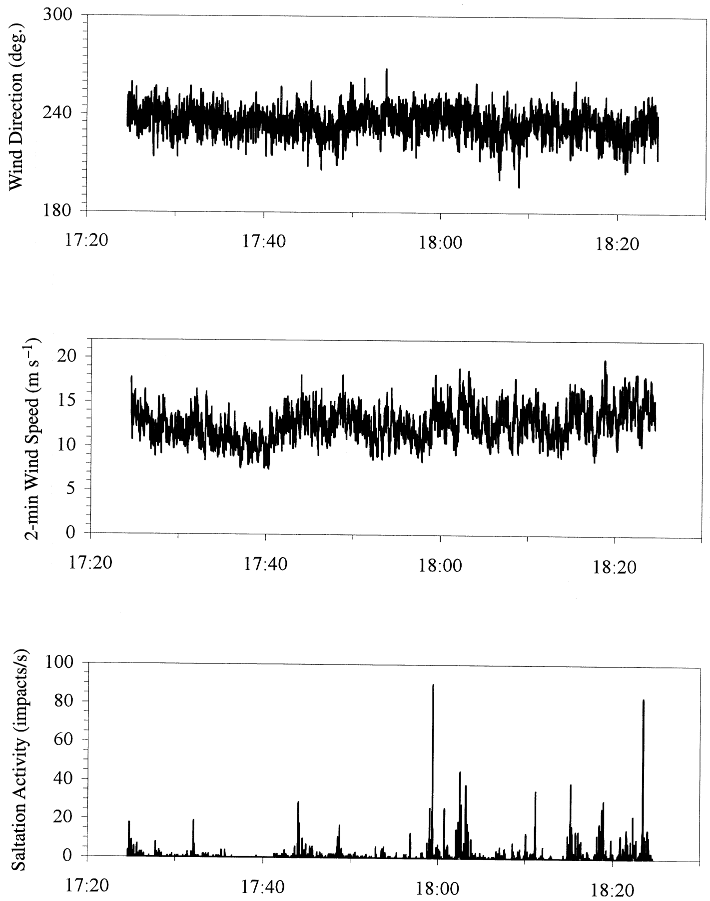

Fig. 6. Wind direction, wind speed, and saltation activity measured from 17:24–18:24 on April 19, 1995.

(1 Hz), each 5-min period contained 300 observations each of wind speed and saltation activity. A pair consisting of one value of relative wind strength s and one value of the intermittency function γ_p was calculated for each 5-min period.

The choice of a 5-min period represents a compromise. If we shorten the period then we obtain more values of s and γ_p per hour. However, since we are sampling at a fixed rate of 1 Hz, reducing the period also reduces the number of observations within each period. With regard to statistical analyses, more observations provide a more statistically valid sample size. This consideration is especially important when calculating the wind distribution. Thus, a 5-min period provides a reasonably large number of observations for statistical analyses yet allows one to calculate 12 values of relative wind strength and γ_p per hour.

Analysis of wind data

Using wind measurements taken during this experiment, we have calculated the probability that the wind speed $u(t)$ is greater than a reference wind speed U, denoted here by $P(u(t)>U)$. We will later look at the more specific situation where U is equal to the threshold u_t of the surface but here we wish to define the form of the wind speed distribution independently of the surface. Calculated wind speed distributions for the first and second hour are shown in Figs 9 and 10, respectively. Note that each plot contains 12 separate 5-min distributions plotted as a function of the nondimensional ordinate $(U-\overline{u})/\sigma$, where $\overline{u}$ is the 5-min mean wind speed and σ is the 5-min standard deviation. Values of $\overline{u}$ and σ calculated for each five-minute period are compiled in Table 2.

The standard normal distribution function is plotted as a solid line in Figs 9 and 10. A comparison reveals that the calculated 5-min wind distribution values follow closely the normal distribution.

To further test whether the winds follow a normal distribution, we have calculated the skewness S_k and the kurtosis K for each 5-min period, as shown in Table 2. Skewness S_k provides a relative measure of the asymmetry of the distribution and is defined as

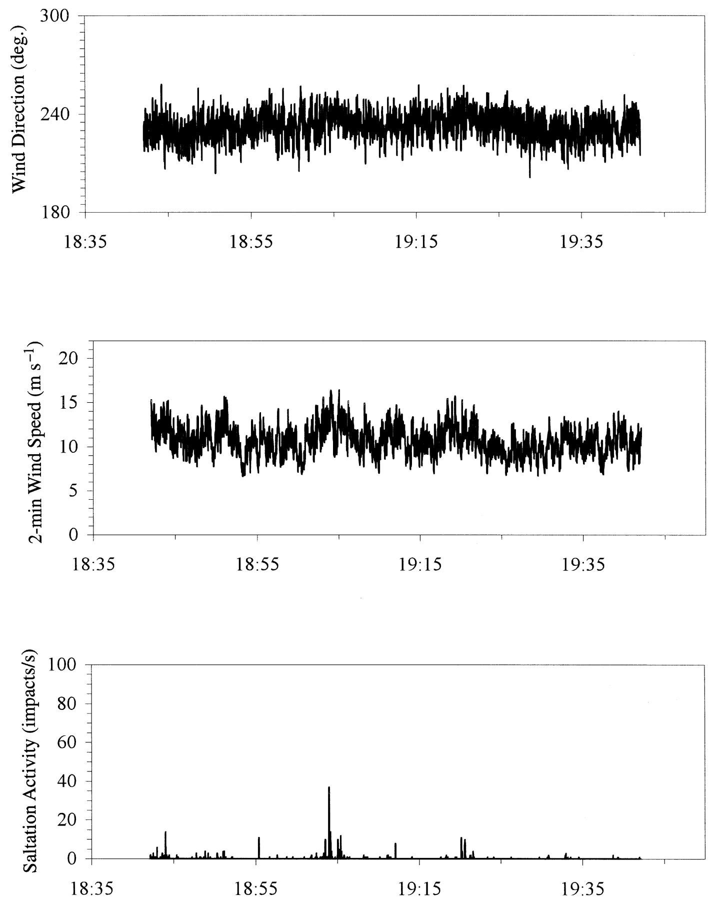

Fig. 7. Wind direction, wind speed, and saltation activity measured from 18:42–19:42 on April 19, 1995.

$$S_k \equiv \frac{\overline{(u(t)-\bar{u})^3}}{\sigma^3}. \tag{9}$$

Kurtosis K characterizes the relative peakedness or flatness of the distribution compared to the normal distribution and is defined as

$$K \equiv \frac{\overline{(u(t)-\bar{u})^4}}{\sigma^4}. \tag{10}$$

A normal distribution has a skewness equal to zero and a kurtosis equal to three (Townsend, 1947).

Calculated values of S_k and K, shown in Table 2, deviate slightly from the ideal normal distribution. The deviations are most likely caused by inhomogeneities of turbulent energy within the boundary layer shear flow and also due to non-stationarity of the turbulent winds (Sutton, 1949; Townsend, 1956; Lumley & Panofsky, 1964; Kuo & Corrsin, 1971). Yet the deviations are not so large as to justify the introduction of a completely different form such as the Weibull or lognormal distribution.

Calculation of the intermittency function

To test the theory put forward in this paper we calculated values of the intermittency function γ_p and values of the relative wind strength s from the measured wind and saltation records. The raw data set consists of three essential columns: time t, the 2-m wind speed $u(t)$, and SENSIT particle impacts per second $p(t)$. Again, we divide the data set into 5-min periods which contain 300 lines of data each. Values of the intermittency function γ_p are constructed from an intermittency signal, $b_p(t)$, defined as

$$\begin{aligned} b_p(t)&=0 \quad \text{if} \quad p(t)=0 \\ b_p(t)&=1 \quad \text{if} \quad p(t)>0 \end{aligned} \tag{11}$$

The fraction of time that saltation is detected γ_p is simply the average value of $b_p(t)$ taken over each 5-min period or

$$\gamma_p = \frac{1}{N}\sum_{i=1}^{N} b_{p_i} = \overline{b_p(t)}, \tag{12}$$

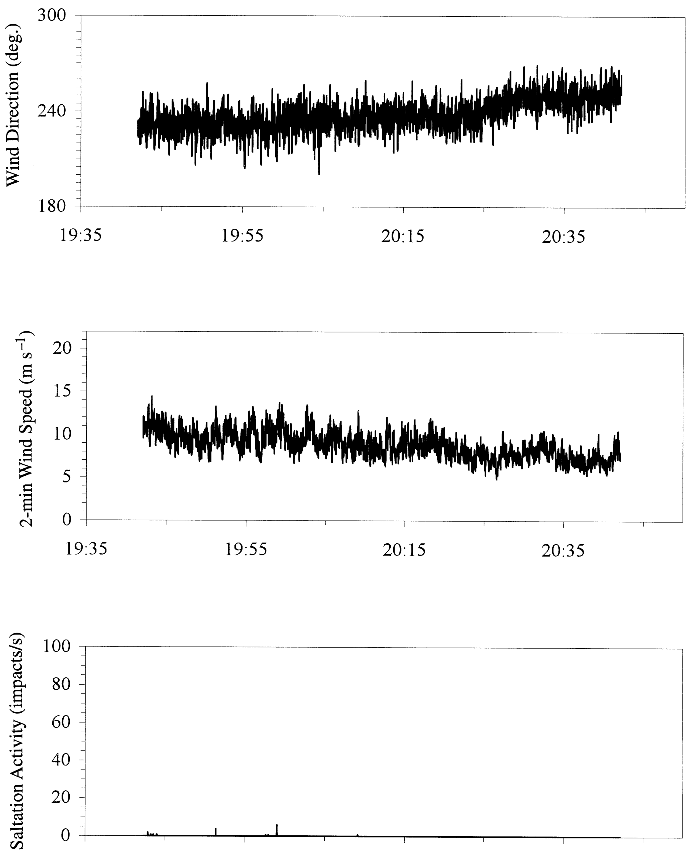

Fig. 8. Wind direction, wind speed, and saltation activity measured from 19:42–20:42 on April 19, 1995.

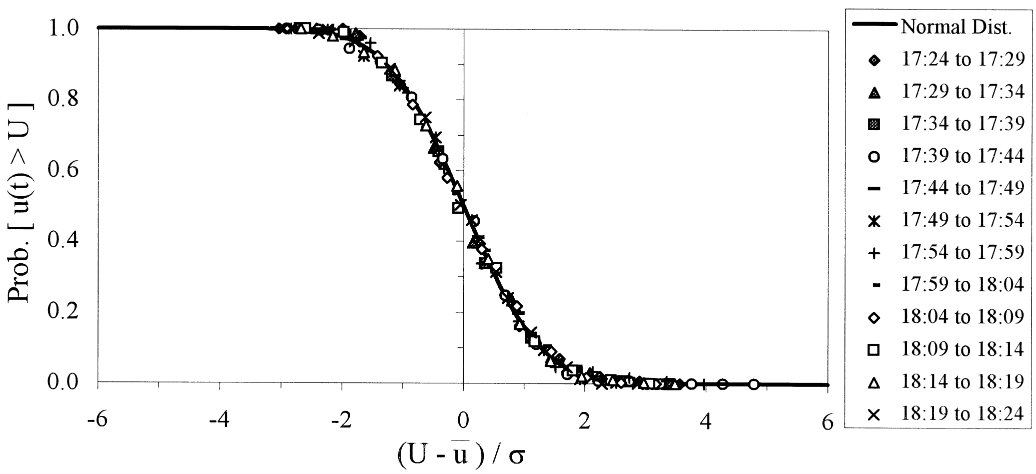

Fig. 9. Plot of wind distribution values calculated for each 5-min interval during the first sampling period (17:24–18:24). Solid line is the normal distribution function.

where N=300. Values of γ_p calculated in this way are compiled in Table 2.

Calculation of threshold

To calculate values of relative wind strength s from our measurements we need to establish the threshold wind speed. A value of threshold can be obtained by requiring the fraction of time that saltation occurs to be equivalent to the fraction of time that winds exceed threshold (Stout & Zobeck, 1996). We simply have to determine by iteration the value of threshold that yields this equivalence. First we make an initial guess for the threshold value u_t and construct an intermittency signal for wind speed as

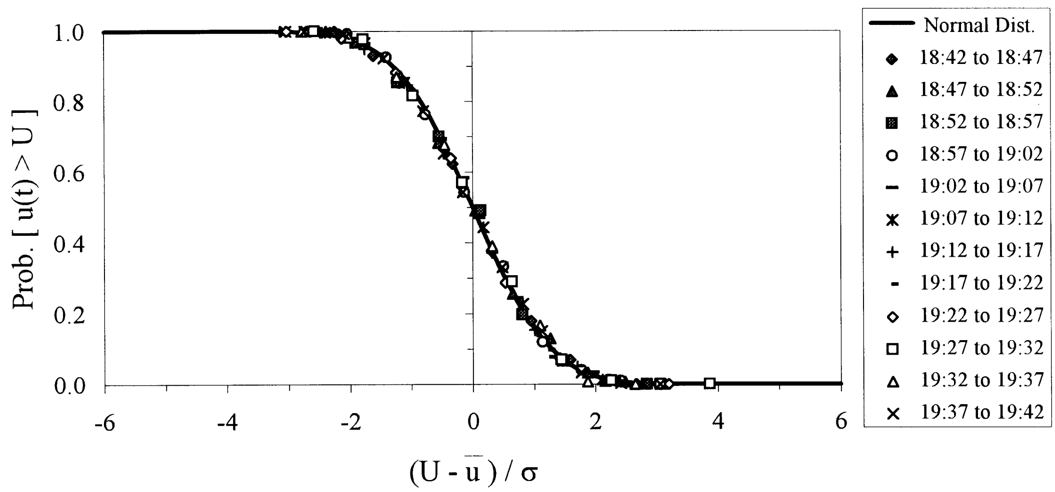

Fig. 10. Plot of wind distribution values calculated for each 5-min interval during the second sampling period (18:42–19:42). Solid line is the normal distribution function.

Table 2. Values of wind direction, mean wind speed $\overline{u}$, standard deviation of wind speed σ, turbulence intensity i, skewness S_k, kurtosis K, threshold wind speed u_t, relative wind strength s, and intermittency function γ_p calculated for each 5-minute subinterval.

time	dir (deg)	$\overline{u}$ (ms^{-1})	σ (ms^{-1})	i	S_k	K	u_t (ms^{-1})	s	γ_p
17:24 to 17:29	239·4	12·60	1·51	0·12	0·37	2·98	13·55	−0·63	0·240
17:29 to 17:34	236·4	11·76	1·55	0·13	0·43	2·79	13·57	−1·17	0·130
17:34 to 17:39	234·8	10·54	1·31	0·12	0·28	3·05	13·30	−2·11	0·033
17:39 to 17:44	233·4	12·16	1·95	0·16	−0·17	2·94	13·84	−0·86	0·203
17:44 to 17:49	232·3	13·13	1·50	0·11	0·07	2·75	13·83	−0·46	0·313
17:49 to 17:54	239·1	12·27	1·68	0·14	−0·17	2·51	13·63	−0·81	0·217
17:54 to 17:59	237·5	12·02	1·63	0·14	0·63	3·95	13·55	−0·94	0·170
17:59 to 18:04	237·8	13·53	1·96	0·14	0·29	2·51	13·73	−0·10	0·450
18:04 to 18:09	230·0	12·67	1·74	0·14	0·18	2·36	14·27	−0·92	0·207
18:09 to 18:14	234·8	12·43	1·58	0·13	0·17	2·44	13·85	−0·89	0·200
18:14 to 18:19	234·0	13·51	1·95	0·14	−0·04	3·03	13·69	−0·09	0·460
18:19 to 18:24	231·2	14·38	1·71	0·12	−0·06	2·72	14·23	0·09	0·523
18:42 to 18:47	229·1	11·52	1·56	0·14	0·11	2·54	13·20	−1·08	0·130
18:47 to 18:52	230·1	11·43	1·64	0·14	0·17	2·51	13·64	−1·35	0·093
18:52 to 18:57	232·6	10·00	1·48	0·15	−0·14	2·48	13·00	−2·03	0·013
18:57 to 19:02	232·4	10·21	1·57	0·15	0·14	2·47	13·60	−2·15	0·027
19:02 to 19:07	236·6	12·33	1·61	0·13	0·05	2·61	13·63	−0·81	0·217
19:07 to 19:12	232·9	10·72	1·55	0·14	0·04	2·50	13·30	−1·66	0·047
19:12 to 19:17	233·7	10·54	1·45	0·14	0·09	2·74	13·80	−2·26	0·013
19:17 to 19:22	237·2	11·72	1·44	0·12	0·13	2·67	13·60	−1·31	0·093
19:22 to 19:27	235·1	9·60	1·12	0·12	0·06	2·83	12·50	−2·58	0·010
19:27 to 19:32	230·0	9·70	1·24	0·13	−0·04	2·53	12·40	−2·17	0·013
19:32 to 19:37	229·0	10·59	1·29	0·12	−0·12	2·33	12·86	−1·76	0·020
19:37 to 19:42	231·5	10·25	1·55	0·15	0·07	2·37	13·55	−2·12	0·013

$$\begin{aligned} b_u(t)&=0 \quad \text{if} \quad u(t)<u_t \\ b_u(t)&=1 \quad \text{if} \quad u(t)\geq u_t \end{aligned} \tag{13}$$

The fraction of time γ_u that the 2-m wind speed exceeds the chosen value of threshold is simply the average value of $b_u(t)$ or

$$\gamma_u=\frac{1}{N}\sum_{i=1}^{N} b_{u_i}=\overline{b_u(t)}. \tag{14}$$

If $\gamma_u>\gamma_p$ then u_t is increased so that γ_u is reduced. If $\gamma_u<\gamma_p$ then u_t is decreased so that γ_u is increased. This process is repeated over many

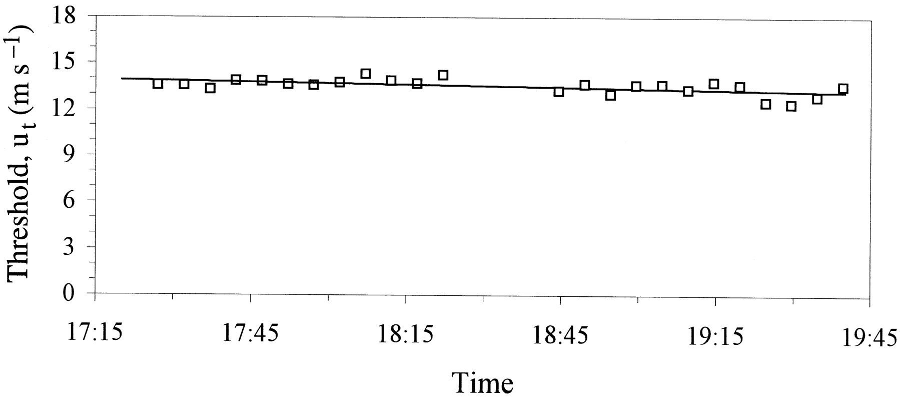

Fig. 11. Calculated values of threshold wind speed plotted as a function of time.

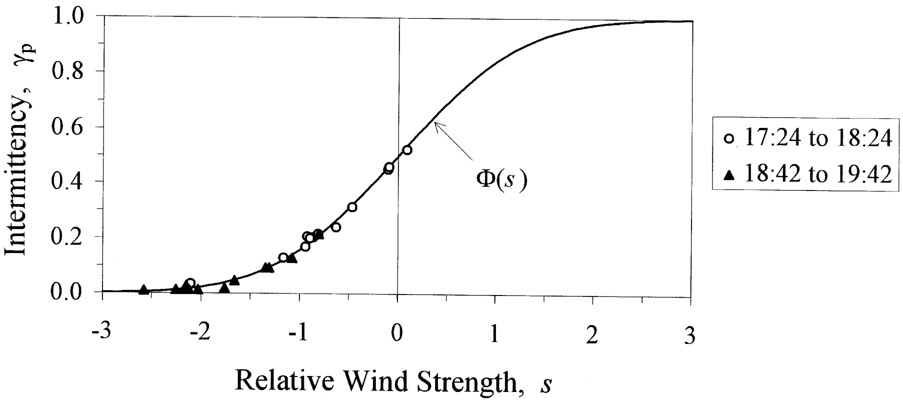

Fig. 12. Plot of the intermittency function γ_p as a function of the relative wind strength *s*. Solid line represents the standard normal distribution function $\Phi(s)$.

iterations until $\gamma_u = \gamma_p$. The final value of u_t that satisfies this equality is considered to be threshold. This method, called the 'time fraction equivalence method,' provides a simple and quantitative means for calculating threshold. Values of threshold calculated by the time fraction equivalence method are presented in Table 2.

Both the value of intermittency γ_p and the value of threshold u_t determined by this method are influenced by the sensitivity of the instrument that detects saltation activity. Here, threshold is defined as the minimum 2-m wind speed which yields saltating grains in excess of the momentum threshold of 5×10^{-8} N s.

Values of threshold calculated by the time fraction equivalence method are plotted as a function of time in Fig. 11. This method appears to yield a fairly consistent value of threshold but there is a slight downward trend with respect to time. Fitting a line to the data, we find that the slope is $-0{\cdot}3$ m s^{-1} h^{-1}. This may indicate that as the storm progressed, the breakdown of surface crusts and clods by the bombardment of saltating grains was producing a smoother surface with more loose erodible material; a surface that was becoming slightly more erodible with time. This type of change in erodibility has been observed by Gillette *et al.* (1996) at Owens Lake, California. Another possibility is that the performance of the anemometer was degraded with time as the bearings became 'sanded'. Marginally degraded bearings could cause the cup assembly to turn more slowly for the same wind speed causing an apparent reduction in threshold that is not real.

Calculation of relative wind strength

Now that we have obtained the mean and standard deviation of the wind speed and calculated threshold, we have sufficient information to calculate the relative wind strength *s* for each 5-min period. The results are compiled in Table 2.

Using the calculated values from Table 2, the intermittency function γ_p is plotted as a function of *s* in Fig. 12. These data are well represented by the normal distribution function which is plotted as a solid line in Fig. 12. Unfortunately there were few positive values of *s* so that only half the curve has been confirmed.

CONCLUSIONS

This field experiment has demonstrated that during a fairly intense wind erosion event, saltation can be very intermittent, characterized by sporadic bursts of blowing soil that occupy a small fraction of the total time. During this experiment, saltation activity rarely accounted for more than 50% of any 5-min period and toward the end of the storm, intermittency values often fell below 2%. Clearly saltation activity occupied a small fraction of the total storm period.

Although there is much more work required to better understand the complex interaction between the wind and soil, we have managed to describe the level of intermittency by a simple and universal mathematical expression. We find that the level of intermittency is directly related to a nondimensional parameter we call the relative wind strength *s*. The relative wind strength is simply the ratio of the difference between the mean wind speed and threshold divided by the standard deviation of the wind speed during the same time period. If relative wind strength *s* is positive then the mean wind speed is greater than threshold and saltation activity would occasionally cease when the wind speed dips beneath threshold. If *s* is negative then the mean wind speed is less than threshold and only occasional gusts exceed threshold and produce blowing soil. We find that the level of intermittency can be described by a simple distribution function of the relative wind strength.

ACKNOWLEDGMENTS

We gratefully acknowledge the assistance and dedication of H. Dean Holder for constructing equipment used in this experiment and for assisting in the field experiment. We would also like to thank Dr Stephen Wolfe, Dr William Porch, Dr Kenneth Pye, and Dr Nicholas Lancaster for carefully reviewing this manuscript.

REFERENCES

Anderson, R.S. and Haff, P.K. (1991) Wind modification and bed response during saltation of sand in air. *Acta Mechanica (Suppl.),* **1,** 21–51.

Bagnold, R.A. (1941) *The Physics of Blown Sand and Desert Dunes.* Methuen, London, 265 pp.

Butterfield, G.R. (1991) Grain transport in steady and unsteady turbulent airflows. *Acta Mech. (Suppl.),* **1,** 97–122.

Butterfield, G.R. (1993) Sand transport response to fluctuating wind velocity. In: *Turbulence: Perspectives on Flow and Sediment Transport* (Ed. by N. J. Clifford, J. R. French and J. Hardisty), pp. 305–335. John Wiley & Sons, New York.

Corrsin, S. (1943) *Investigation of the flow in an axially symmetrical heated jet of air.* NACA Wartime Report W–94.

Corrsin, S. and Kistler, A.L. (1954) *The free-stream boundaries of turbulent flows.* NACA Technical Note 3133.

Fiedler, H. and Head, M.R. (1966) Intermittency measurements in the turbulent boundary layer. *J. Fluid Mech.,* **25,** 719–736.

Gillette, D.A. and Stockton, P.H. (1986) Mass, momentum and kinetic energy fluxes of saltating particles. In: *Aeolian Geomorphology* (Ed. by W. G. Nickling), pp. 35–56. Allen and Unwin, Boston.

Gillette, D.A., Herbert, G., Stockton, P.H. and Owen, P.R. (1996) Causes of the fetch effect in wind erosion. *Earth Surface Processes and Landforms.,* **21,** 641–659.

Heathershaw, A.D. and Thorne, D.D. (1985) Sea-bed noises reveal the role of turbulent bursting phenomenon in sediment transport by tidal currents. *Nature,* **316,** 339–342.

Jackson, D.W.T. (1996) A new, instantaneous aeolian sand trap design for field use. *Sedimentology,* **43,** 791–796.

Justus, C.G., Hargraves, W.R. and Yalcin, A. (1976) Nationwide assessment of potential output from wind-powered generators. *J. Appl. Meteor.,* **15** (7), 673–678.

Kawamura, R. (1951) *Study on sand movement by wind.* Institute of Science and Technology, Tokyo, Report 5, pp. 95–112.

Kuo, A.Y. and Corrsin, S. (1971) Experiments on internal intermittency and fine-structure distribution functions in fully turbulent fluid. *J. Fluid Mech.,* **50** (2)**,** 285–319.

Lee, J.A. (1987) A field experiment on the role of small scale wind gustiness in aeolian sand transport. *Earth Surface Processes and Landforms,* **12,** 331–335.

Lumley, J.L. and Panofsky, H.A. (1964) *The Structure of Atmospheric Turbulence.* Interscience Publishers, New York.

Luna, R.E. and Church, H.W. (1974) Estimation of long term concentrations using a 'universal' wind speed distribution. *J. Appl. Meteor.,* **13,** 910–916.

Maitani, T. (1979) A comparison of turbulence statistics in the surface layer over plant canopies with those over several other surfaces. *Boundary-Layer Meteorol.,* **17,** 213–222.

McEwen, I.K. and Willetts, B.B. (1991) Numerical model of the saltation cloud. *Acta Mechanica (Suppl.),* **1,** 53–66.

Porch, W.M. (1974) Fast-response light scattering measurements of aerosol suspension in a desert area. *Atmos. Env.,* **8,** 897–904.

Simmons, L.F.G. and Salter, C. (1934) Experimental investigation and analysis of the velocity variations in turbulent flows. *Proc. Roy. Soc. A,* **145,** 212–234.

Sorbjan, Z. (1989) *Structure of the Atmospheric Boundary Layer.* Prentice Hall, New Jersey. 317 pp.

Sørensen, M. (1991) An analytical model of wind-blown sand transport. *Acta Mechanica (Suppl.),* **1,** 67–81.

Stockton, P. and Gillette, D.A. (1990) Field measurements of the sheltering effect of vegetation on erodible land surfaces. *Land Degradation and Rehabilitation,* **2,** 77–85.

Stout, J.E. and Zobeck, T.M. (1996) Establishing the threshold condition for soil movement in wind-eroding fields. In: *Proceedings of the International Conference on Air Pollution from Agricultural Operations,* pp. 65–71. MidWest Plan Service (MWPS C-3), Kansas City, 7–9 February 1996.

Sutton, O.G. (1949) *Atmospheric Turbulence.* Methuen, London.

Takle, E.S. and Brown, J.M. (1978) Note on the use of Weibull statistics to characterize wind-speed data. *J. Appl. Meteor.,* **17,** 556–559.

Thorne, P.D., Williams, J.J. and Heathershaw, A.D. (1989) In situ measurements of marine gravel threshold and transport. *Sedimentology,* **36,** 61–74.

Townsend, A.A. (1947) The measurement of double and triple correlation derivatives in isotropic turbulence. *Proc. Camb. Phil. Soc.,* **43** (4)**,** 560–570.

Townsend, A.A. (1956) *The Structure of Turbulent Shear Flow.* Cambridge University Press, London.

Weibull, W. (1951) A statistical distribution function of wide applicability. *J. Appl. Mech.,* **18,** 293–297.

Zingg, A.W. (1953) *Wind tunnel studies of the movement of sedimentary material.* Proceedings 5th Hydraulic Conference Bulletin, **34,** 111–35.

Manuscript received 10 April 1996; revision accepted 24 December 1996.